Numerical Simulation of NACA 4412 Airfoil to Analysis its Performance Characteristics

Md. Ahatashamul Haque Khan Shuvo[1]*, Nabbo Solila Nodee[2], and Md. Atikur Rahman[3]

[1-3]Department of Mechanical Engineering, Sonargaon University, Dhaka, Bangladesh

*E-mail: mahskhan.khan@gmail.com

Abstract

Investigations on the NACA 4412 airfoil are performed to analyze the influence of ground effect and angle of attack dispersion. The aim is to enhance our comprehension of these phenomena and assess their efficacy in relation to aerodynamic variables. The experimental plan utilizes ANSYS 15 and is based on a three-level factorial design of experiments. The objective is to construct a regression model for the lift to drag (L/D) ratio. There is no correlation observed between ground clearance and angle of attack in relation to both L/D ratio and coefficient of moment. It is revealed by the coefficient of moment,a strong negative impact of component B. Nevertheless, this study solely validates the boundaries that were examined. The model provides us with the optimal L/D ratio and coefficient of moment. At a zero-degree angle of attack, the values are CL 0.53436 and CD 0.00093215, while at an eight-degree AOA, the values are CL 1.4494 and CD 0.0095451. Estimating the value has advantages for designing and testing the NACA 4412 airfoil within specified boundaries.

Keywords: *Turbulent Flow Model, Pressure Contour, Velocity Contour, Velocity Vector, Angle of Attack*

1.0 INTRODUCTION

The work is partitioned into three studies. Initially, the efficacy of the numerical tools is examined through the simulation of an airfoil in a state of constant and unchanging flight. The simulations are performed by solving the incompressible Angle of Attack (AOA) and employing the correlation-based transition model to predict the flow of the transitional boundary layer. Following that, a method for enhancing the airfoil is developed and assessed to reduce the decrease in efficiency caused by contamination at the front edge of wind turbine blades. Ultimately, a technique for enhancing winglet performance is created and evaluated for a small-scale wind turbine model. The equations are solved to mimic the performance of the turbine, and an airfoil surrogate model is constructed to determine the winglet that performs the best. In order to enhance the surrogate, a hybrid genetic-gradient optimization technique is used to maximize an infill criterion that is based on expected improvement [1]. The wind tunnel is used to validate the efficacy of the simulated wind turbine, both with and without winglets, through experimental testing. The initial section of the study reveals that the airfoil's performance is significantly underestimated when the transitional boundary layer flow is omitted. This highlights the crucial significance of accurately simulating the dynamics of fluid flow [2,3]. Research has demonstrated that when optimizing airfoils and winglets for wind turbine use, global evolutionary algorithms generate solutions that are either equivalent to or better than the current state of technology [3-5].

A fluid flowing across an airfoil-shaped body generates an aerodynamic force. Lift is described as the component that acts normal to the trajectory of motion. Drag is a term that describes the component that is aligned with the direction of motion. Evaluating the impact of aerodynamics on the NACA 4412 2D airfoil, Manga discovered that the static pressure is stronger at the front edge compared to the negligible pressure at the rear. The velocity component indicates that the air on the lower surface of the blade must cover a greater distance in a given amount of time compared to the air on the top surface [6]. Subsonic flight airfoils exhibit a distinctive form featuring a curved front edge, followed by a pointed rear edge, often displaying symmetrical curvature on both upper and lower surfaces. Hydrofoils are water-based foils that serve a similar purpose [7]. The lift generated by an airfoil is predominantly influenced by its AOA and its form. When the airfoil is positioned at the correct angle, it redirects the incoming air, resulting in a force on the airfoil that counteracts the redirection. The aerodynamic force can be broken down in two constituent parts named lift and drag. Observations indicate that the lift coefficient rises as the angle of attack increases until reaching specific thresholds, beyond which it declines due to flow separation [8]. Most types of foil require a positive AOA to provide lift, however cambered airfoils can generate lift even when the AOA is null. The rotation of the air around the airfoil generates curved streamlines, leading to decreased pressure on bottom and increased pressure on top. Hocine [9] discovered that the Tapered form exhibits an enhanced lift coefficient and reduced drag coefficient compared to the rectangular shape at all AOA. The pressure difference between the top and bottom surfaces of the airfoil leads to a difference in velocity, as explained by Bernoulli's principle. Consequently, the flow of air around the surface of airfoil, the upper one has a higher mean velocity compared to the lower one. The lift force is directly proportional to the difference in average velocity between the top and bottom surfaces by utilizing the principles of circulation and the theorem by Kutta-Joukowski [10,11].

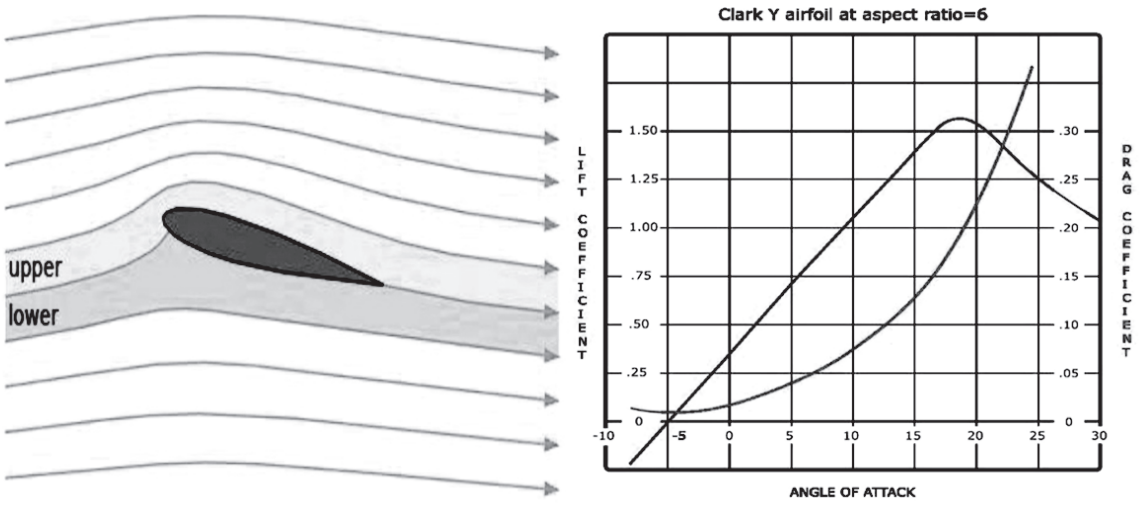

(a) (b)

Fig. 1: (a) Flow patterns around a NACA 0012 at a modest AOA (b) Drag and lift curve for a standard airfoil [12]

2.0 DERIVATION OF THIN AIRFOIL THEORY

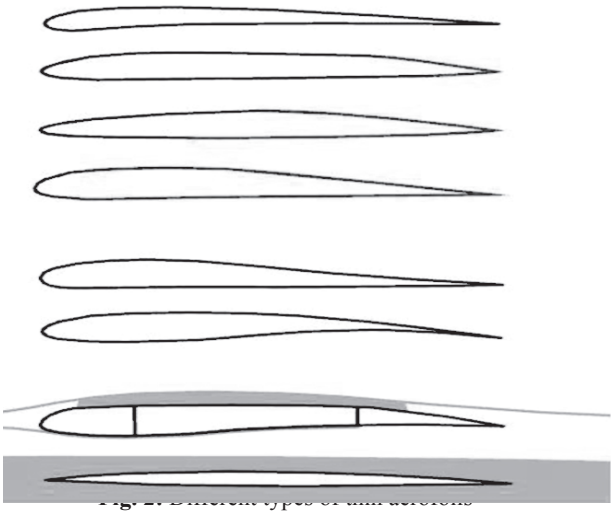

Vertically we find:

- Aerofoil for laminar flow in
  - » RC park flyer
  - » RC pylon racer
  - » Manned propeller aircraft
  - » Airfoil for Jet airliner
- Steady airfoil commonly employed in aircraft wings.
- Airfoil designed to accommodate a heavy load, which enables the use of a big main spar and delays the onset of stall
- Aerofoil for transonic supercritical aircraft
- Aerofoil for supersonic leading-edge type aircrafts

Colors in the aerofoils:
Black represents laminar flow, Red indicates turbulent flow, Grey means subsonic stream, Blue shows supersonic flow volume.

$$V\left(\alpha - \frac{dy}{dr}\right) = w(x) = \frac{1}{(2\pi)}\int_{\circ}^{c} \frac{\gamma(x')}{(x - x')}dx'$$

Solving this integral equation for x, replacing x by $x - c\dfrac{1 - cost(\theta)}{2}$

as a Fourier A_n sin (nθ) series in with an altered lead, term

$$A_{\circ}\frac{1 + \cos(\theta)}{\sin(\theta)}$$

That is: $$\frac{\gamma(\theta)}{(2V)} = A_{\circ}\frac{1 + \cos(\theta)}{\sin(\theta)} + \sum A_n \sin(n\theta)$$

These are identified as Glauert integral. The coefficients are,

$$A_{\circ} = \alpha - \frac{1}{\pi}\int_{\circ}^{\pi}\left(\frac{dy}{dx}\right)\, d\theta$$

and $$A_n = \frac{2}{\pi}\int_{\circ}^{\pi}\cos(n\theta)\left(\frac{dy}{dx}\right)\, d\theta$$

By the Kutta–Joukowski theorem, the total lift force, denoted as F, is directly proportional to

$$\rho V\int_{\circ}^{c}\gamma(x)dx$$

and moment M is calculated for the leading edge is

$$\rho V\int_{\circ}^{c}x\gamma(x)dx$$

The computed Lift coefficient is solely determined by the initial two elements of the Fourier series, as

$$CL = 2\pi\left(A_{\circ} + \frac{A_1}{2}\right)$$

At the leading edge, moment M is solely dependent on A0;A1 and 2 , as

$$C_M = -0.5\pi\left(A_{\circ} + \frac{A_1}{2}\right)$$

About the 1/4 chord point, the moment will thus be,

$$C_M\left(\frac{1}{4c}\right) = \frac{\pi}{4}(A_1 - A_2)$$

It is found that the center of pressure is aft of the 'quarter-chord' point 0.25 c, by

$$\Delta\frac{x}{c} = \frac{\pi}{4}\frac{A_1 - A_2}{CL}$$

The aerodynamic center, AC, is at the quarter-chord point where the pitching moment M' does not vary with angle of attack, i.e.,

$$\frac{\partial(C_M')}{\partial(C_L)} = 0$$

Equation of drag is given by, $Fd = \dfrac{1}{2}rn^2Cd$

so co efficient of drag is given by the, $Cd = \dfrac{2Fd}{rn^{2A}}$

This implies that the drag force on an object is directly related to the fluid density as well as the square of its relative velocity. Coefficient of drag, denoted by Cd, is a dimensionless number that identifies an object's resistance aka drag in a fluid medium like air or water. The drag equation measures aerodynamic efficiency by calculating the drag coefficient. A lower number indicates less drag. Drag coefficients constantly depend on the surface area. In fluid dynamics, skin friction and form drag determine an object's drag coefficient. Airfoil and hydrofoil lift-induced drag is included in their drag coefficients. Aircraft drag includes interference drag. Traditional drag measurements use the drag coefficient. Drag coefficient determines reference area. The reference area for cars and other items is the predicted frontal area.

3.0 AIRFOIL PROFILES DESIGNATION

National Aeronautics Advisory Committee produced aeroplane wing profiles called NACA airfoils. The numbers after "NACA" represent the airfoil configuration. The numerical code can be utilized to develop numerical equations that define the cross-sectional area of an aerofoil and estimate the characteristics. The airfoil configurations proposed by NACA are four digit, five digit, and modified 4-/5-digit, were developed using scientific comparisons that analyze the curvature of the geometric centerline of the airfoil section and the spread of thickness along its length. Subsequently, throughout the period from 2013 to 2015, ambiguous forms were deduced using speculative methods about the 6-Series [13-15]. Before NACA introduced these arrangements, the design of airfoils was mostly based on arbitrary shapes, with limited knowledge of recognized shapes and investigation of alterations to certain structures.

3.1 Flows on Airfoil: Types

A laminar flow is defined by the presence of air layers, or laminas, that move at a constant speed at the same direction. There is no exchange of fluid between the layers, and the flow does not need to be in a linear path. The laminas' velocity decreases as they approach the surface of the airfoil. The flow of a perfect liquid follows after the bended surface readily, in laminas. For turbulent flows, the flow patterns become disordered and exists a significant interchange of liquid between different regions. Momentum is exchanged in a manner where sluggish liquid particles gain speed while particles that move quickly transfer their energy to the sluggish ones and subsequently gets slowed down. Almost every liquid flow exhibits some degree of turbulence. [16,17].

The Reynolds number is a fundamental parameter for studying fluid dynamics, especially in relation to the boundary layer. Streams with similar Reynolds numbers exhibit similar behaviour. It can be calculated using the precise formula. If a moderate level of precision is acceptable, the Reynolds number can be estimated using the equation provided below:

$Re = \nu \times l \times 70000$

Where: “ν” represents the speed of flight
“L” ” represents length of chord in m.
70000 is the constant value for air with unit $\left(\frac{s}{m^2}\right)$

Reynolds number is determined based on the chord length of an aerofoil (measured in 2D) or the wing chord length. The mean aerodynamic chord length is used to represent the Reynolds number for a wing, as the chord length can vary from the root to the tip. Various types of airflow include subsonic (Mach number M < 0.1), transonic, and supersonic flows across the airfoils. Similarly, the fluid might be classified as compressible, incompressible, or inviscid [17-19].

3.2 Inviscid Flow Model

The curves of lift and drag coefficient are computed at various angles of attack using the turbulence model for NACA 4412.

Table 1: Coefficient of lift and coefficient of drag values obtained with inviscid model

Angle of Attack (AoA)	Coefficient of Lift (C_L)	Coefficient of Drag (C_D)
0°	0.53436	0.00093215
8°	1.4494	0.0095451

Within the realm of aviation, the term "angle of attack" (AOA) pertains to the angle formed between the incoming airflow and a designated reference line on an aircraft or its wings. Occasionally, the line of reference is a line that connects the foremost edge with the subsequent edge at a specific halfway on the wing. This is the situation that occurs in extraordinary circumstances. The lift coefficient (CL) and drag coefficient (CD) were measured at a zero-degree angle, resulting in values of 0.53436 and 0.00093215, respectively. Occasionally, the angle of attack (AOA) is mistakenly identified as either the pitch angle or the flight path angle (see Table 1). The angle in question is visually depicted on the attitude indicator, also known as the false horizon, as seen in figures 3 to 5. Figure 4 provides a visual representation of the angle of the flight path when the aircraft encounters either a headwind or a falling air mass.

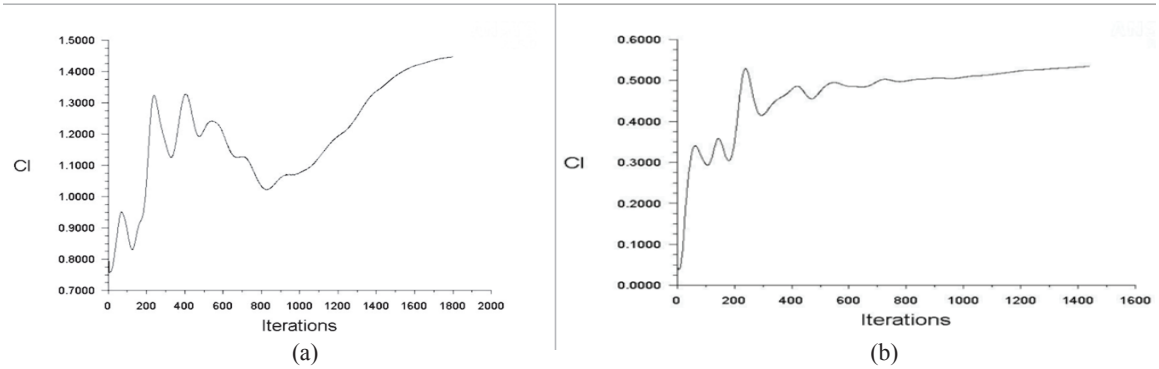

(a) (b)

Fig. 3: Convergence of CL for (a) α=0° and (b)α=8°

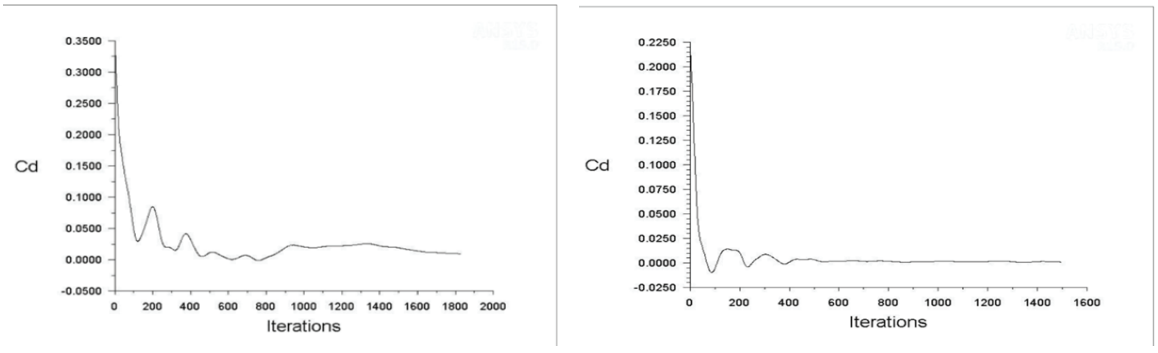

(a) (b)

Fig. 4: Convergence of C_d for (a) α=0° and (b)α=8°

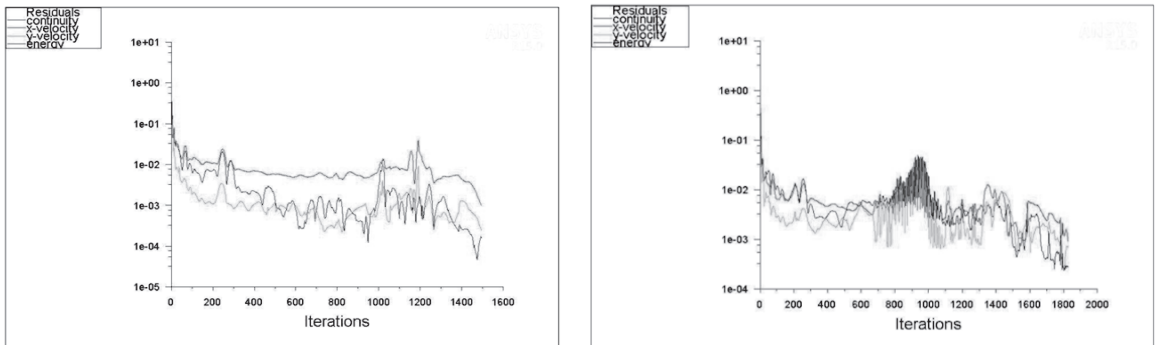

(a) (b)

Fig. 5: Residuals for (a) α=0° and (b)α=8°°

4.0 CONTOURS

4.1 Pressure Contour

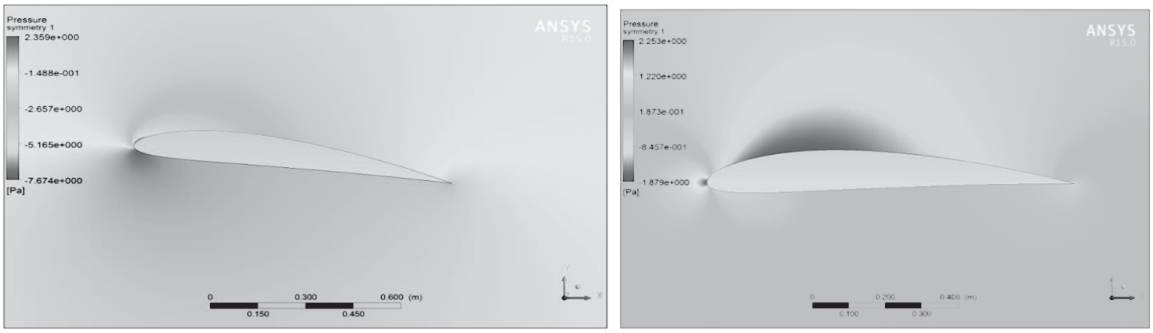

(a) (b)

Fig. 6: (a)Contour of Pressure (α=0°), (b)Contour of Pressure (α=8°)

The static pressure contours at different attack angles were produced for NACA 4412 in figures 6 (a) and (b). The figures display the results of CFD analysis. The flow velocity is increased on the upper side of each airfoil, while it is reversed on the lower side. Hence, the lift coefficient will see a rise, as will the drag coefficient. On the other hand, the amount of the increase in lift is far greater than the magnitude of the rise in drag. The pressure differential between the lower and top surfaces of each airfoil favors higher pressure on the lower surface. Every airfoil experiences an upward force that effectively counteracts the entering flow stream.

4.2 Velocity Contour

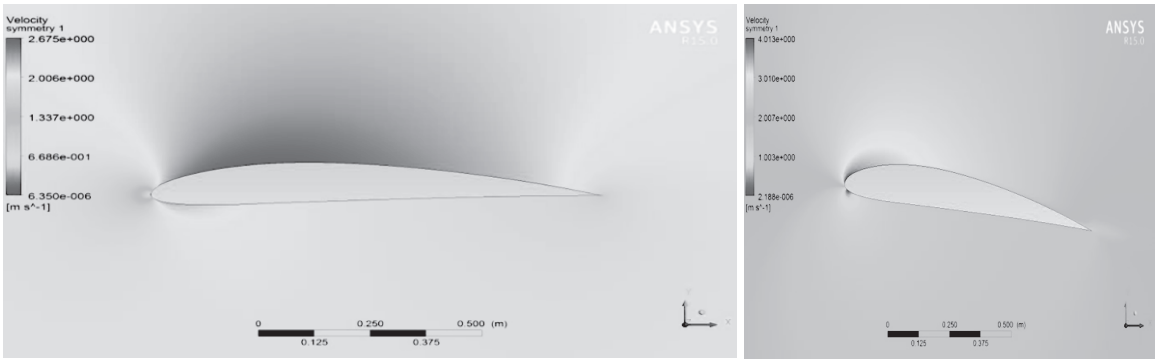

(a) (b)

Fig. 7: (a) Contour of Velocity (α=0°), (b)Contour of Velocity (α=8°)

The velocity contours at different attack angles were produced for NACA 4412 in figures 7 (a) and (b). These figures depict the results of CFD simulationsWe find the stagnation point at the leading edge, which is the point at which the airflow velocity is almost not moving at all for each and every airfoil. For each aerofoil, with the increase in flow velocity for the upper surface, the flow velocity completely reverses for the lower surface.

4.2 Velocity Vectors

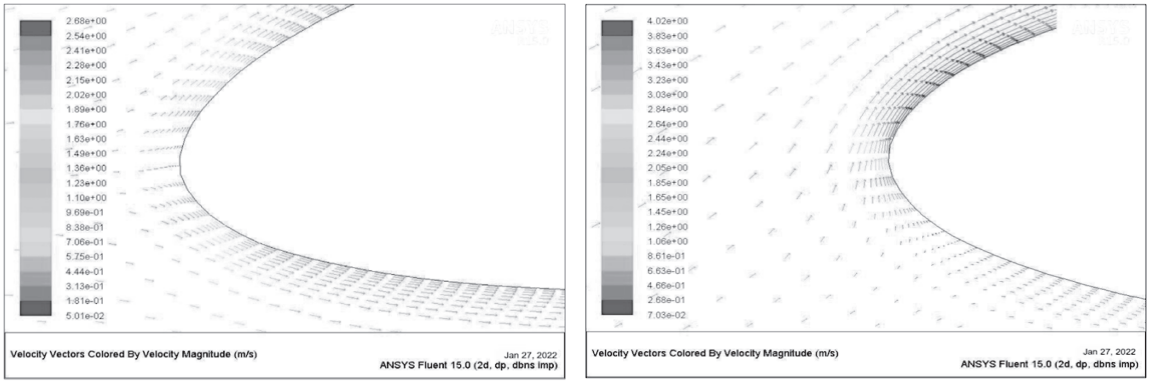

(a) (b)

Fig.8: Velocity Vectors (α=0°), (b) Velocity Vectors (α=8°)

The velocity on the both sides of the airfoil is almost equal when the angle of attack is zero, as depicted in Figure 8 (a) and (b). When the angle of attack reaches 10 degrees, the fluid begins to separate and creates wakes. As a result, pressure drag occurs. At an AOA of 16 degrees, the separation of airflow achieves its greatest value, and subsequently, the lift begins to decrease.

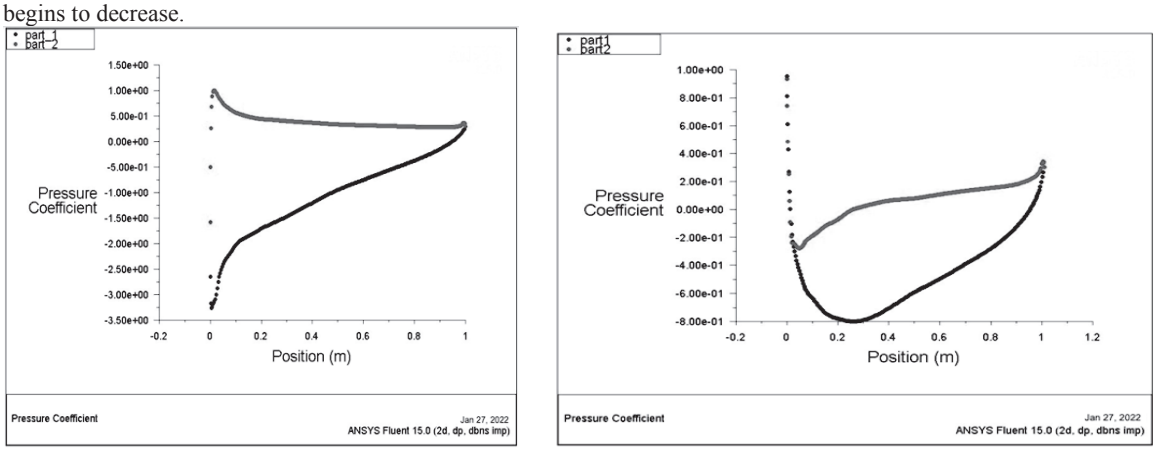

(a) (b)

Fig. 9: (a) Coefficient of Pressure (α=0°) (b)Coefficient of Pressure (α=8°)

5.0 SPALART ALLMARAS TURBULENT FLOW MODEL

In aerodynamics applications, it is essential for all airfoils to generate a significant amount of lift while minimizing drag to achieve optimal performance. It is important to do a comparative analysis of various airfoils in order to choose the most efficient one. One can also acquire this data by graphing CL and CD against various angles of attack. Simulation results indicate that the lift to drag ratio increases as the AOA increases. This relationship is observed in figures 10-12. The lift to drag ratio is a performance metric used to evaluate the efficiency of airfoils. Designing aircraft often involves prioritizing this as one of the primary objectives. The table provides the values of the lift and drag coefficient for the NACA 4412 airfoil.

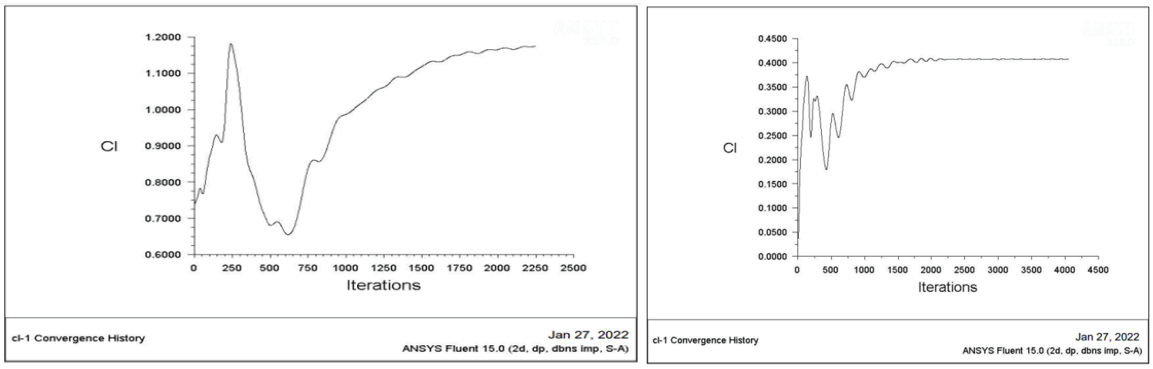

(a) (b)

Fig. 10: (a) Convergence of CL Plot against Number of Iterations (α=0°), (b) Convergence of CL Plot against Number of Iterations (α=8°)

Table 2: Coefficient of Lift and Coefficient of Drag Allmaras Model

Angle of Attack (AoA)	Coefficient of Lift (C_L)	Coefficient of Drag (C_D)
0°	0.40727	0.018226
8°	1.1790	0.031933

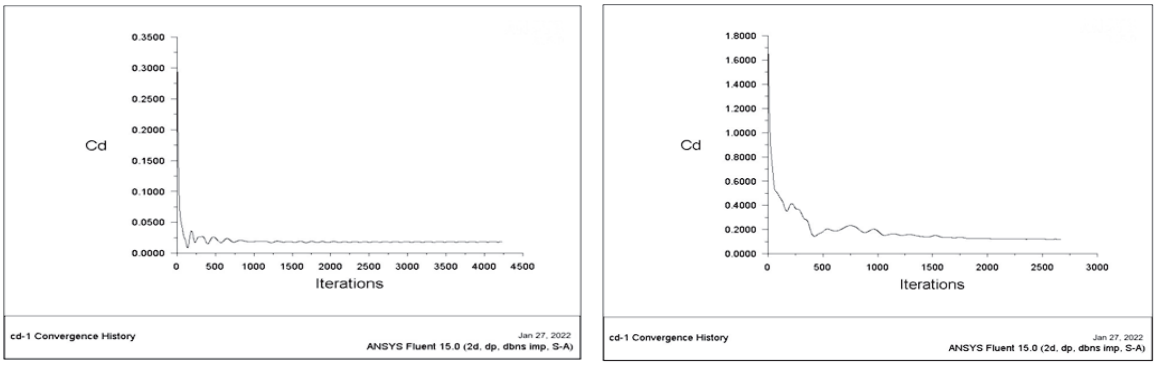

(a) (b)

Fig. 11 : (a) Convergence of CD Plot against Number of Iterations (α=0°), (b) Convergence of CD Plot against Number of Iterations (α=8°).

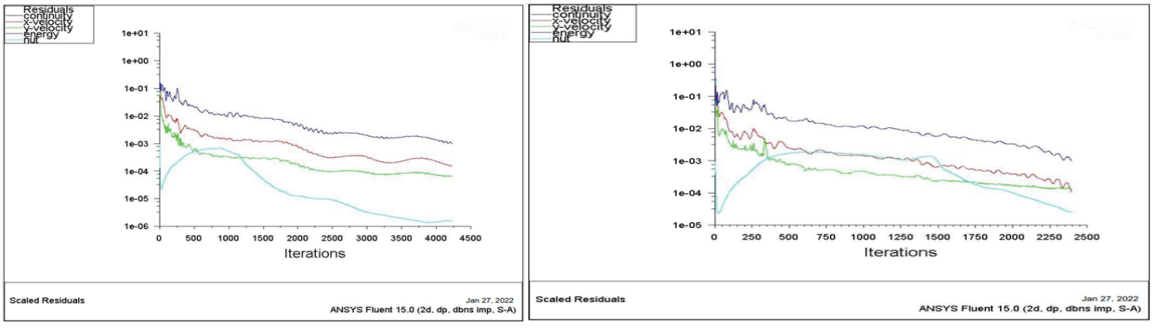

(a) (b)

Fig. 12 :: Convergence of Residual Plots against Number of Iterations (α=0°), Convergence of Residual Plots against Number of Iterations (α=8°)

6.0 CONCLUSION

An investigation on the aerodynamic efficiency of the NACA 4412 airfoil has been conducted at different attack angles (0°, 8°) under constant conditions, while also considering the influence of the turbulence model. These calculations will facilitate the computation of the overall power coefficient of a turbine. This airfoil can also be utilized in other turbine stations or radial locations. From the velocity magnitude data, it is evident that the flow velocity at the top surface is greater than the flow velocity at the bottom surface. Furthermore, the flow velocity on the upper surface increases as the attack angles increase. It is evident from the static pressure contours that the static pressure on the lower surface of the airfoil rises as the attack angles increase. From the pressure coefficient values, it is evident that the upper surface of the airfoil exhibits a negative pressure coefficient, while the bottom surface displays a positive pressure coefficient. Consequently, the lift force acting on the airfoil is directed upwards. It is evident from the tables of CL and CD values that as the attack angles rise, the values of CL and CD also increase. Upon examination of the CL/CD values, it is evident that the optimal AOA for NACA 4412 is 6°. Upon analyzing the static pressure contours of NACA 4412, it becomes evident that this airfoil exhibits a higher pressure gradient at all angles of attack.

[1] D.Rana, S.Patel, AK.Onkar and M.Manjuprasad, "Time domain simulation of airfoil flutter using fluid structure coupling through FEM based CFD solver", Symposium of Apllied Aerodynamics and Design of Aerospace vehicle, SAROD20111, Nov 16-18 2009, Bangalore.

[2] T. Gultop , "An Investigation of the effect of aspect ratio on Airfoil performance", Gazi : American Journal of Applied Sciences, Vol: 2, Issue: 2: 545-549 ,1995.

[3] M.Arvind "CFD Analysis of Static Pressure and Dynamic Pressure For NACA 4412" International Journal of Engineering Trends and Technology ISSN/EISSN: 22315381 Volume: 4 Issue: 8 Pages: 3258-3265, (2010).

[4] P. Panagiotou, K. Yakinthos, "Aerodynamic efficiency and performance enhancement of fixed-wing UAVs", Aerospace Science and Technology, Vol.99, pp.105575 (1-13), 2020.

[5] Pranto, M.R.I. and Inam, M.I., "Numerical Analysis of the Aerodynamic Characteristics of NACA4312 Airfoil", Journal of Engineering Advancements, 1(02), pp.29-36, 2020..

[6] P.J Manga, Adisa A. Bello, M.A Tijjani, Felix W. Burari, M.A Abdull Azeez, P.B Teru, Yukubu Nura, R.O Amusat, Garba Ibrahim, & S. Daniel., "Two-dimensional analyses based computational fluid dynamics on NACA 4412 airfoil", Nigerian Journal of Sustainable Research, 1(1), 1-9, 2023.

[7] M. Kevadiya (2013)" CFD Analysis of Pressure Coefficient for NACA 4412" International Journal of Engineering Trends and Technology ISSN/EISSN: 22315381 Volume: 4 Issue: 5 Pages: 2041-2043, 2013.

[8] MB. Arnab, MI. Inam, "Comparison of Aerodynamic Performance of NACA 23012 and NACA 4412 Airfoil: A Numerical Approach", International Conference on Mechanical, Industrial and Energy Engineering, Khulna, Bangladesh, 2022.

[9] H. Hares, G. Mebarki, "Influence of Wing Shape on Airfoil Performance: a Comparative Study", Wseas Transactions On Fluid Mechanics, Volume 18, 2023.

[10] N. Ahmed, B.S. Yilbas, M.O. Budair;" Computational study into the flow field developed around a cascade of NACA 0012 airfoils". Comput. Methods Appl. Mech. Engrg. 167 (1998) 17-32.

[11] MS Arif, MJ Afzal, F. Javaid, S, Tayyaba, MW Ashraf, GFI Toki, MK Hossain, "Laminar Flow Analysis of NACA 4412 Airfoil Through ANSYS Fluent", 8th International Exchange and Innovation Conference on Engineering & Sciences, 2022.

[12] Kunz, P. J., Kroo, I.,Analysis, "Design and testing of airfoils for use at ultra-low Reynolds numbers, Proceedings of the Conference on Fised, Flapping and Rotary Vehicles at very Low Reynolds Numbers", edited by T. J. Mueller, Univ. of Notre Dame, Notre Dame, IN, pp.349-372, 2000.

[13] S. Mittal and P. Saxena; "Hysteresis in flow past a NACA 0012 airfoil". Comput. Methods Appl. Mech. Engrg. 191 2179– 2189, 2002

[14] Shrestha, B., & Bhattarai, N.,"Numerical Simulation Studies on Stall Suppression of a NACA0015 Airfoil", Journal of Advanced College of Engineering and Management, 6, 23-31, 2021.

[15] Roul, R., Studies on Performance of an Airfoil and Its Simulation (Doctoral dissertation), 2015.

[16] B. Ravi Kumar, "Enhancing aerodynamic performance of NACA 4412 aircraft wing using leading edge modification", Wind and Structures, Vol.29, No.4, 2019, pp.271-277.

[17] S. Obeid, R. Jha, G. Ahmadi, RANS, "Simulations of Aerodynamic Performance of NACA 0015 Flapped Airfoil", Fluids. 2 (2017) 2.

[18] Md. I. K. Monirul, A. Al-Faruk, "Comparative analysis of aerodynamic characteristics of rectangular and curved leading edge wing planforms", American Journal of Engineering Research, Vol.7, No.5, 2018, pp.281-291.

[19] Husain Mehdi, Vipul Namdev, Prashant Kumar, Ashish Tyagi, "Numerical Analysis of Fluid Flow around a Circular Cylinder at Low Reynolds Number", IOSR, Journal of Mechanical and Civil Engineering, vol 3, issue 3, 2016, 94-101.